Winter December, 2010

High switching endurance in TaOxTaOx memristive devices

Jianhua Yang, *University of Massachusetts - Amherst*
M Zhang
John Strachan
Feng Miao
Matthew Pickett, et al.

High switching endurance in TaO_x memristive devices

J. Joshua Yang, M.-X. Zhang, John Paul Strachan, Feng Miao, Matthew D. Pickett, Ronald D. Kelley, G. Medeiros-Ribeiro, and R. Stanley Williams

We demonstrate over 1×10^{10} open-loop switching cycles from a simple memristive device stack of $Pt/TaO_x/Ta$. We compare this system to a similar device stack based on titanium oxides to obtain insight into the solid-state thermodynamic and kinetic factors that influence endurance in metal-oxide memristors.

Memristive devices have attracted significant attention because of their great potential for next generation nonvolatile memory,[1,2] stateful logic operations via material implication,[3] neuromorphic computing,[4] and a variety of complementary metal-oxide semiconductor (CMOS)/memristor hybrid circuits.[5,6] Accordingly, significant progress has been made in understanding the physical operating mechanisms as well as in improving the device performance,[7–22] leading to the demonstration of nonvolatility, fast switching (<10 ns), low energy (~1 pJ/operation), multiple-state operation, scalability, stackability, and CMOS compatibility for these devices. However, one of the major challenges for memristors to be used in a universal memory (e.g., replacing DRAM as well as Flash) or as a Boolean computing device is endurance,[1,7] i.e., how many cycles the devices can reversibly and reliably switch. The endurance values reported in the literature range from 10 to 1×10^6 cycles and the endurance record has been 1×10^9 cycles so far.[19] Here we demonstrate that the endurance limit of metal-oxide memristive devices has not yet been reached. We have achieved over 1×10^{10} switching cycles [see Fig. 1(a)] in a very simple $Pt/TaO_x/Ta$ device stack while using fixed switching parameters in an open circuit without any feedback mechanism. The device remains functional even after 15×10^9 cycles. We have compared TiO_x- and TaO_x-based memristors with a similar device structure and observed a significantly better endurance in the latter. Based on these observations and the known phase diagrams for the Ti–O and Ta–O systems, we discuss some criteria for material selection to achieve high endurance.

The structure of the Ta oxide devices is schematically shown in the inset to Fig. 1(b). The TaO_x film was sputter-deposited from a tantalum oxide target with an Ar working gas pressure of about 3 mTorr. The resulting film had a composition of $TaO_{1.7}$ based on Rutherford backscattering spectrometry characterizations, whereas the nominal composition of the target was $TaO_{2.0}$. The substrate was Si with a 200 nm thermal SiO_2 film and the device stack typically included a blanket Pt bottom electrode of 100–400 nm, a blanket TaO_x layer of about 7–18 nm, and a Ta metal top electrode of 100–400 nm. A very thin (1 nm) Ti layer was used between the Pt bottom electrode and the substrate for adhesion purpose. The Ta top electrode had a disk shape with a diameter of 100 μm, defining the device area. This simple device stack was designed to meet the main structural requirements for a high endurance device: (1) the Ta metal electrode serves as a large reservoir of mobile dopant species (O vacancies or possibly Ta interstitials) for the electronic switching, (2) the asymmetry of the two interfaces defines a stable switching polarity, (3) the thick metal electrodes serve as heat sinks and also provide low electrode series resistance, (4) the built-in oxygen deficiency protects the device from gas eruption damage,[12] (5) the planar structure mitigates the edge effects of a crossbar structure, and (6) the blanket oxide layer effectively isolates the key junction for switching (the chemically inert TaO_x/Pt interface) from air.

The typical switching current-voltage (I-V) loops of the TaO_x devices are shown in linear and also semilog scales in Fig. 1(b). The devices switch at a relatively low voltage, which is highly desirable for sub-20 nm CMOS drive circuitry. The switching current is less than 100 μA even though the device area is very large. The voltage for the first set operation [green I-V in Fig. 1(b)] is only slightly larger than the subsequent normal set (i.e., device off to device on)

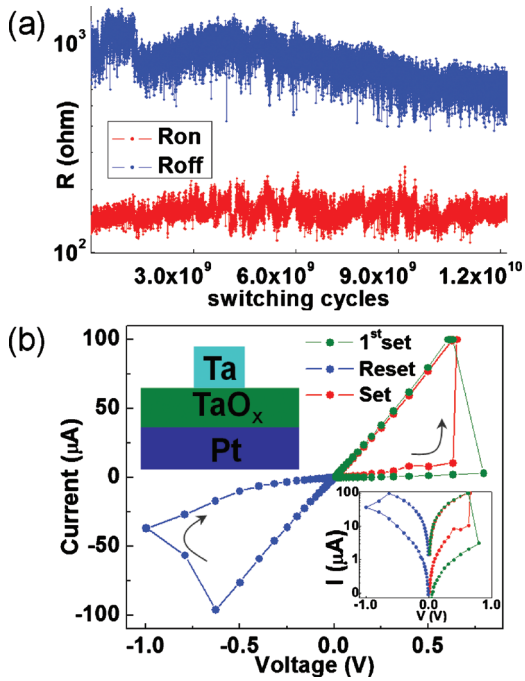

FIG. 1. (Color) (a) The endurance and (b) typical switching I-V loops of a simple $Pt/TaO_x/Ta$ device stack.

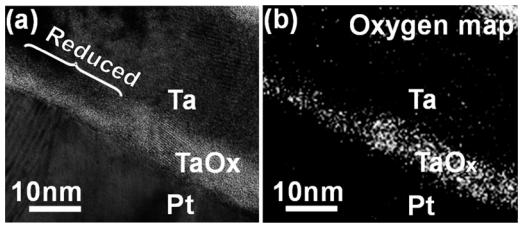

FIG. 2. (a) The EFTEM zero-loss image and (b) oxygen map of the switching region for the cross section of a Pt/TaO_x/Ta device.

switching, suggesting that no dramatic electroforming is required for the device operation. Over 1×10^{10} switching cycles are shown in Fig. 1(a) [the first 1×10^{9} cycles are shown in Fig. 3(b)] for which fixed voltage pulses of 1 μs with about +1.9 V (voltage drop across the devices) for set and −2.2 V for reset were used for the endurance test in Fig. 1(a). The voltages were applied on the Ta top electrode and the Pt bottom electrode was grounded in all the measurements. Because of the parasitic capacitance from the wires and cables, 1 μs pulses were used in the experiments reported here, although we have observed sub-10 ns switching using a high bandwidth fixture and cabling. The devices retained their resistance state after three months at room temperature without significant degradation and are still undergoing endurance and lifetime experiments.

We utilized pressure modulated conductance microscopy[12,23] to locate the localized active switching region within the device area and then prepared a cross-sectional sample for transmission electron microcopy (TEM) through this active region using focused ion beam. The energy-filtered TEM (EFTEM) zero-loss images and oxygen map of the switching region are shown in Figs. 2(a) and 2(b), respectively. The result from Fig. 2 is that the Ta oxide film thickness in the switching region was significantly reduced after the electrical operations. The original thickness of the TaO_x film was about 7 nm, but within the active region of the device, this thickness is reduced by half as shown in Fig. 2(a). Additionally, it can be seen from Fig. 2(b) that the oxygen content in the reduced region is almost as low as that in the deposited Ta top electrode.

The equilibrium solid-phase diagram for the Ta–O system is quite simple; there are only two stable phases for temperatures under 1000 °C:[24] the single-metal-valence compound Ta_2O_5 and Ta metal, which can have a few percent of dissolved O and is denoted by Ta(O). However, there are a large number of metastable phases, including one with the stoichiometry TaO_2 that has the rutile structure. The Ta oxide material deposited by sputtering was electrically insulating and had an overall stoichiometry of $TaO_{1.7}$, and from our TEM analyses was primarily amorphous with some nanocrystal inclusions of Ta_2O_5. The thin conducting region found in the film was likely formed by phase separation of the metastable deposited material into a thin Ta_2O_{5-x} layer and Ta(O) by joule heating, although there is some possibility of solid-state electrochemical reduction during the first set pulse.

In order to further explore the role of the switching material system in the endurance performance of memristive devices, we prepared Ti oxide devices with a similar device stack to the schematic in Fig. 1(b). A pure Ti metal top electrode was found to result in an almost electrically short device using TiO_2 as the switching material because of the

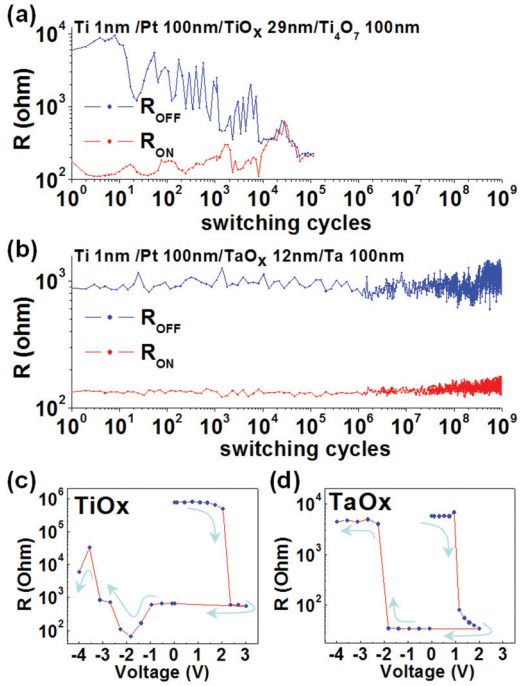

FIG. 3. (Color) Comparison of TiO_x and TaO_x devices. Endurance of the (a) TiO_x device and (b) TaO_x device. Resistance changes under 1 μs voltage pulses with increasing voltage magnitude for the (c) TiO_x device and (d) TaO_x device.

significant reaction to yield more Ti rich stable phases. Therefore, a Ti_4O_7 metallic film was used as the top electrode, and a thicker TiO_2 active layer was used compared to the TaO_x device because there are many stable oxides (the Magnéli phases[25]) with a higher O content than Ti_4O_7, so it is still possible for the TiO_2 to be reduced by this metallic oxide electrode layer. Typical endurance results from the TiO_x and TaO_x devices are presented in Figs. 3(a) and 3(b), respectively. Large fluctuations were observed in both the on and off resistance states of the TiO_x device, where the window between on and off states quickly collapsed. The device was not shorted after the collapse and it could be refreshed to reset resistance window again by applying a larger voltage pulse than that used for the endurance test. In contrast, the TaO_x device exhibited fairly stable on and off states for over 1×10^{9} switching cycles using fixed amplitude voltage pulses, as shown in Fig. 3(b).

The endurance performance difference between these two samples is most likely related to the thermodynamic differences in these two oxide systems, only two stable phases in the Ta–O system[24] but a large number, especially an entire series of Magnéli phases, in the Ti–O system.[25] For the Ti oxide system, the mechanism of memristive switching involves the drift of positively charged oxygen vacancies (V_Os) into and out of an insulating interfacial region under the applied electric field.[26,27] The growth and retraction of a conductive channel(s) in the insulating matrix result in the low and high resistance states.[27,28] The conductance channel is a suboxide phase, e.g., Ti_4O_7 (Refs. 8 and 14) that acts as a source/sink of vacancies for an insulating TiO_2 matrix, which is where the switching actually occurs. The as-prepared sputtered film in the Ta oxide device was amorphous with a nominal composition of $TaO_{1.7}$, which is an inhomogeneous metastable insulating material.

Working by analogy to the much better understood Ti oxide system, it is likely that the active region of the Ta oxide device phase separates and forms regions of the two stable phases of the Ta–O system under joule heating during the device burn-in stage of the first set operation. The Ta_2O_5 can serve as the insulating matrix and the Ta(O) solid solution can serve as the conductance channel and the effective source of mobile dopant species. These two phases are nominally in thermodynamic equilibrium, meaning they will not react with each other even under an elevated temperature caused by joule heating in the devices. As a result, the device can sustain a large voltage amplitude without any significant chemical changes.

This is demonstrated in Figs. 3(c) and 3(d), showing the resistance changes of the devices under accumulating voltage pulses of different amplitudes. Each blue data point represents a 1 μs electrical pulse, with the bottom scale of the plots representing the voltages applied (external voltages), which are larger than the internal voltage drops across the devices. Starting from a high resistance off state, the devices were first set by positive voltage pulses with an increasing voltage magnitude. At an apparent voltage threshold of +1 V for the TaO_x device in Fig. 3(d) (which since these are dynamical devices, will be different for different pulse widths), the device was quickly set to a low resistance on state. Then the pulses were inverted in polarity to negative voltages, and starting from the on state, the resistance increased at -2 V and then remained in a fairly stable off state despite a large overdrive with negative voltage pulses. In sharp contrast, the TiO_x device exhibited an unstable reset switching behavior under increasing negative voltage pulses, as can be seen in Fig. 3(c), where the resistance of the device first decreased, then increased to the off state, but decreased again under overdrive conditions. We attribute this unstable behavior to the fact that the conductive channel material is not in equilibrium with the insulating matrix material in the TiO_x device and complicated chemical reactions continue to be activated by joule heating when overdriven. However, a slight overdrive is necessary in endurance tests in order to compensate for the variance in the effective write threshold voltage from cycle to cycle and avoid bit errors during writing, which thus has a negative impact on the endurance for the TiO_x device.

It is notable that in the literature, the two cases where 1×10^9 switching cycles have been reported in oxide switches are in the Ta–O (Ref. 19) and Hf–O (Refs. 22) systems. These two binary systems share the same features, namely, only two stable solid phases in bulk equilibrium with each other, one of which is insulating and the other is a conducting phase (the metal) with a large oxygen solubility, which can act as the source/sink of mobile ions for switching in the insulating phase. For oxide systems without these features, such as WO_x and TiO_x, a sophisticated feedback mechanism to avoid overdriving[29] or an additional step of refreshing of the devices with stronger voltage pulses[30] were needed in order to obtain a lower record endurance in the range of 10×10^6 switching cycles.

We thank J. Borghetti, X. Li, W. Yi, J. Nickel, T. Ha, and C. Le for excellent experimental assistance. This work is supported in part by the U.S. Government's Nano-Enabled Technology Initiative.

[1] A. Chung, J. Deen, J. S. Lee, and M. Meyyappan, Nanotechnology **21**, 412001 (2010).
[2] D. B. Strukov, G. S. Snider, D. R. Stewart, and R. S. Williams, Nature (London) **453**, 80 (2008).
[3] J. Borghetti, G. S. Snider, P. J. Kuekes, J. Joshua Yang, D. R. Stewart, and R. Stanley Williams, Nature (London) **464**, 873 (2010).
[4] T. Hasegawa, T. Ohno, K. Terabe, T. Tsuruoka, T. Nakayama, J. K. Gimzewski, and M. Aono, Adv. Mater. **22**, 1831 (2010).
[5] Q. F. Xia, W. Robinett, M. W. Cumbie, N. Banerjee, T. J. Cardinali, J. J. Yang, W. Wu, X. M. Li, W. M. Tong, D. B. Strukov, G. S. Snider, G. Medeiros-Ribeiro, and R. S. Williams, Nano Lett. **9**, 3640 (2009).
[6] J. Borghetti, Z. Y. Li, J. Straznicky, X. M. Li, D. A. A. Ohlberg, W. Wu, D. R. Stewart, and R. S. Williams, Proc. Natl. Acad. Sci. U.S.A. **106**, 1699 (2009).
[7] R. Waser, R. Dittmann, G. Staikov, and K. Szot, Adv. Mater. **21**, 2632 (2009).
[8] D. H. Kwon, K. M. Kim, J. H. Jang, J. M. Jeon, M. H. Lee, G. H. Kim, X. S. Li, G. S. Park, B. Lee, S. Han, M. Kim, and C. S. Hwang, Nat. Nanotechnol. **5**, 148 (2010).
[9] R. L. McCreery and A. J. Bergren, Adv. Mater. **21**, 4303 (2009).
[10] S. C. Chae, J. S. Lee, S. Kim, S. B. Lee, S. H. Chang, C. Liu, B. Kahng, H. Shin, D. W. Kim, C. U. Jung, S. Seo, M. J. Lee, and T. W. Noh, Adv. Mater. **20**, 1154 (2008).
[11] S. H. Jo, K. H. Kim, and W. Lu, Nano Lett. **9**, 496 (2009).
[12] J. J. Yang, F. Miao, M. D. Pickett, D. A. A. Ohlberg, D. R. Stewart, C. N. Lau, and R. S. Williams, Nanotechnology **20**, 215201 (2009).
[13] M. D. Pickett, D. B. Strukov, J. L. Borghetti, J. J. Yang, G. S. Snider, D. R. Stewart, and R. S. Williams, J. Appl. Phys. **106**, 074508 (2009).
[14] J. P. Strachan, M. D. Pickett, J. J. Yang, S. Aloni, A. L. David Kilcoyne, G. Medeiros-Ribeiro, and R. Stanley Williams, Adv. Mater. **22**, 3573 (2010).
[15] J. Yao, L. Zhong, Z. X. Zhang, T. He, Z. Jin, P. J. Wheeler, D. Natelson, and J. M. Tour, Small **5**, 2910 (2009).
[16] E. Linn, R. Rosezin, C. Kugeler, and R. Waser, Nature Mater. **9**, 403 (2010).
[17] C. Schindler, M. Weides, M. N. Kozicki, and R. Waser, Appl. Phys. Lett. **92**, 122910 (2008).
[18] M. N. Kozicki, C. Gopalan, M. Balakrishnan, and M. Mitkova, IEEE Trans. Nanotechnol. **5**, 535 (2006).
[19] Z. Wei, Y. Kanzawa, K. Arita, Y. Katoh, K. Kawai, S. Muraoka, S. Mitani, S. Fujii, K. Katayama, M. Iijima, T. Mikawa, T. Ninomiya, R. Miyanaga, Y. Kawashima, K. Tsuji, A. Himeno, T. Okada, R. Azuma, K. Shimakawa, H. Sugaya, I. Takagi, R. Yasuhara, K. Horiba, H. Kumigashira, and M. Oshima, Tech. Dig. - Int. Electron Devices Meet. **2008**, 293.
[20] N. Gergel-Hackett, B. Hamadani, B. Dunlap, J. Suehle, C. Richter, C. Hacker, and D. Gundlach, IEEE Electron Device Lett. **30**, 706 (2009).
[21] K. M. Kim, B. J. Choi, Y. C. Shin, S. Choi, and C. S. Hwang, Appl. Phys. Lett. **91**, 012907 (2007).
[22] H. Y. Lee, P. S. Chen, T. Y. Wu, Y. S. Chen, C. C. Wang, P. J. Tzeng, C. H. Lin, F. Chen, C. H. Lien, and M. J. Tsai, Tech. Dig. - Int. Electron Devices Meet. **2008**, 297.
[23] F. Miao, J. J. Yang, J. P. Strachan, D. Stewart, R. S. Williams, and C. N. Lau, Appl. Phys. Lett. **95**, 113503 (2009).
[24] S. P. Garg, N. Krishnamurthy, A. Awasthi, and M. Venkatraman, J. Phase Equilib. **17**, 63 (1996).
[25] H. Okamoto, J. Phase Equilib. **22**, 515 (2001).
[26] J. J. Yang, J. Borghetti, D. Murphy, D. R. Stewart, and R. S. Williams, Adv. Mater. **21**, 3754 (2009).
[27] J. J. Yang, M. D. Pickett, X. Li, D. A. A. Ohlberg, D. R. Stewart, and R. S. Williams, Nat. Nanotechnol. **3**, 429 (2008).
[28] J. J. Yang, J. P. Strachan, Q. Xia, D. A. A. Ohlberg, P. J. Kuekes, R. D. Kelley, W. F. Stickle, D. R. Stewart, G. Medeiros-Ribeiro, and R. S. Williams, Adv. Mater. **22**, 4034 (2010).
[29] W. C. Chien, Y. C. Chen, E. K. Lai, Y. D. Yao, P. Lin, S. F. Horng, J. Gong, T. H. Chou, H. M. Lin, M. N. Chang, Y. H. Shih, K. Y. Hsieh, and R. Liu, IEEE Electron Device Lett. **31**, 126 (2010).
[30] C. Yoshida, K. Tsunoda, H. Noshiro, and Y. Sugiyama, Appl. Phys. Lett. **91**, 223510 (2007).